Modelling FACTS Controllers in Fast-Decoupled State Estimation

Cristina F. S. Hasler
Elizete M. Lourenço
Odilon L. Tortelli
Federal University of Parana
Department of Electrical Engineering
Curitiba, Brazil

Renan K. Portelinha
Power and Energy Systems
INESC TEC
Porto, Portugal

***Abstract*—This paper proposes to extend the fast-decoupled state estimation formulation to bring its well-known efficiency and benefits to the processing of networks with embedded FACTS devices. The proposed method approaches shunt-, series-, and shunt-series-type devices. The controller parameters are included as new active or reactive state variables, while controlled quantity values are included in the metering scheme of the decoupled approach. From the electrical model adopted for each device, the extended formulation is presented, and a modified fast-decoupled method is devised, seeking to ensure accuracy and impart robustness to the iterative solution. Simulation results conducted throughout the IEEE 30-bus test system with distinct types of FACTS devices are used to validate and evaluate the performance of the proposed decoupled approaches.**

***Index Terms*—Decoupled Methods, FACTS Devices, State Estimation.**

I. Introduction

The current electric energy transmission and distribution scenario presents numerous challenges in the planning and operation stages. Concerning planning, new resources and infrastructures are expected to be optimized to reduce environmental impact, while in terms of operation, it is expected that the electricity supply will be carried out while maintaining the required levels of quality, reliability and safety. The search for solutions to achieve these goals has increased, propelling the installation of advanced equipment on power networks, such as flexible alternating current transmission devices (FACTS). The adoption of these devices is justified by their capabilities to control the power system in multiple terms: power flow, bus voltage, line impedance, power angle, etc [1].

Traditional electrical power system analysis tools must be updated to incorporate adequate modelling of FACTS devices and their *modus operandi* implications. This is crucial for the proper and accurate functioning of the power system state estimator, which needs to ensure a reliable estimate of the current operational state of the power grid [2]-[3].

Submitted to the 23rd Power Systems Computation Conference (PSCC 2024). E. Lourenço thanks the financial support of the Brazilian National Research Council (CNPq) and C. Hasler thanks the support of the Brazilian Agency for the Improvement of High Education (CAPES) – Finance Code 001.

The representation of FACTS devices in the state estimation problem has been the subject of different approaches in the literature. In [4] and [5], for example, the authors include equality and inequality constraints in the nonlinear least squares minimization problem to take into account the classification and operational limits of the Unified Power Flow Controller (UPFC), while the interior point method is used to solve the resulting optimization problem. Constraints were also added to the classic estimation problem in [6] as a way to represent the operational limits of Thyristor Controlled Series Capacitor (TCSC), Static VAR Compensator (SVC) and UPFC. In [7] equality constraints were used to represent the losses associated with the voltage source converter present in the Static Synchronous Compensator (STATCOM) and Voltage Source Converter based High-Voltage Direct Current (VSC-HVDC). In [8], power injection equations are incremented in the classical formulation of the Weight Least Square (WLS) state estimation to model the UPFC. In [9], Unified Interphase Power Controllers (UIPC) devices and their complex power flow equations are considered in the Jacobian of the WLS state estimation algorithm.

Measurements from phasor measurement units (PMU) have also been approached in state estimation problems with FACTS. This is the case of [10], where the authors propose a WLS state estimation formulation, following an object-oriented programming approach and incorporating sparsity techniques that consider the controllers' current and voltage phasor measurements for SVC, TCSC and UPFC. Modifications to the classic formulation in [11] and [12] are also presented as a way to consider PMU measurements in the estimation process. Alternative approaches are found in [13] and [14]. While in [13] the minimum absolute value estate estimation formulation is extended to incorporate the UPFC and it is solved by the primal-dual interior point method, in [14] the authors propose improvements to robust state estimators techniques which contemplate UIPC and IPC devices. Despite several important efforts aiming at the inclusion of FACTS devices into the power system state estimation problem formulation, to the author's best knowledge, fast-decoupled state estimation approaches which include said devices have yet not been addressed.

This work proposes new steady-state modellings and strategies to incorporate shunt-, series-, and shunt-series-type FACTS into the fast-decoupled WLS state estimation, hereafter referred to as FD-SE. It is noteworthy that FD-SE has found wide acceptance in the industry due to its precise solution, with high computational efficiency through the well-known active and reactive partition of the problem and its constant coefficient matrices [3]. Previous efforts of the authors presented in [15], show the viability of incorporating TCSC devices into the FD-SE and have inspired the present work.

The proposed modified FD-SE method is capable of processing networks equipped with different types of FACTS devices. It is based on the inclusion of new state variables that represent the FACTS' parameters, and new non-linear equations, used to model new virtual measurements related to the controlled variables. Modifications in the fast-decoupled approach are proposed to ensure that the usual assumptions are effectively applied to the new set of equations and variables. The resulting tool presents a high level of accuracy and robustness while maintaining the same computational efficiency as the fast-decoupled approach, as discussed in the upcoming sections.

The covered FACTS devices are the Static VAR Compensator (SVC), the Static Synchronous Compensator (STATCOM), the Static Synchronous Series Compensator (SSSC), and the Unified Power Flow Controller (UPFC). Besides providing an estimate of complex bus voltages and control parameters, the proposed methodology can be applied to determine the necessary settings for the FACTS parameters to meet a pre-defined network operating condition of the network.

Applications of the proposed FACTS-embedded state estimator and comparisons with the WLS state estimator are presented and discussed. Simulations are presented for the IEEE 30-bus test system under the presence of distinct FACTS devices and different operating conditions to illustrate and evaluate the proposed approach.

II. Fast-decoupled state estimation: traditional and alternative approaches

State estimation methods based on the Weighted Least Squares (WLS) technique remain widely applied in the industry. In this approach, the state variables are estimated to fit the set of measurements better, modelled as (1) [16]:

$$z = h(x) + e \tag{1}$$

where z is the measurement vector; x is the state vector, composed of the bus voltage phase angles and magnitudes; $h(x)$ is the vector of non-linear functions that relates the measurements with the state variables, and e is the measurement error vector.

In WLS estimation, obtaining an estimate for the state vector, $\hat{x}$, involves solving the optimization problem that aims to minimize the residual between the actual measurements (z) and their estimated values $h(\hat{x})$. Therefore, the state estimation objective function may be presented as in (2), where R is the measurement error covariance matrix [3]:

$$\min J(\hat{x}) = [z - h(\hat{x})]^T R^{-1} [z - h(\hat{x})] \tag{2}$$

The first-order optimality condition leads to the iterative solution of (2) via the following linear system:

$$G(\hat{x})\Delta\hat{x} = [H(\hat{x})]^T R^{-1} [z - h(\hat{x})] \tag{3}$$

where $G(\hat{x})$ is the Gain matrix, given by $G(\hat{x}) = H^T(\hat{x})R^{-1}H(\hat{x})$ and $H(\hat{x})$ is the Jacobian matrix of measured functions, *i.e.*, $H(\hat{x})$=$\partial h(\hat{x})/\partial\hat{x}$. The state vector is updated via $\hat{x}^{i+1} = \hat{x}^i + \Delta\hat{x}$ and iterations proceeds until convergence.

The high computational cost associated with the state estimation solution in (3), dictated mainly by the calculation and factorization of the Gain matrix at each iteration, made room for decoupled methods, which divide the problem into two subproblems with submatrices half the size of the original. The fact that the Gain matrix does not change significantly during the iterative process supported the use of constant matrices, leading to the fast decoupled state estimation method, discussed next.

Fast-decoupled methods are based on the fact that, in high-voltage systems, active power is more sensitive to changes in phase angles, while reactive power is more sensitive to changes in voltage magnitudes. Decoupling is performed on the measurement model (1), in ways that its corresponding arrays, z and $h(\hat{x})$, undergo a partition between active and reactive measurements, that is, z is partitioned into z_P and z_Q, the vectors of the active and reactive measurement values, respectively; and $h(\hat{x})$ into $h_P(\hat{x})$ and $h_Q(\hat{x})$, the active and reactive measurement functions, respectively. This partitioning affects the Jacobian and Gain matrices, which can be rewritten as:

$$H(x) = \begin{bmatrix} H_{P\theta} & H_{PV} \\ H_{Q\theta} & H_{QV} \end{bmatrix} \qquad G(x) = \begin{bmatrix} G_{P\theta} & G_{PV} \\ G_{Q\theta} & G_{QV} \end{bmatrix} \tag{4}$$

where $H_{P\theta}$ and H_{PV} are the derivatives of the active measurement functions to the phase angle and voltage magnitude, respectively, while $H_{Q\theta}$ and H_{QV} are the derivatives of reactive measurement functions to the voltage phase angle and magnitude, respectively.

In the most widespread approach of the fast-decoupled state estimator, the off-diagonal block matrices of the Jacobian matrix, H_{PV} and $H_{Q\theta}$, are neglected, while the diagonal block matrices are kept constant (computed at *flat start*) [16], [3]. This allows the decoupling between the active and reactive subproblems, which are then solved sequentially, by:

Model-Decoupled SE Algorithm (MD-SE):

$$G^{md}_{P\theta}\Delta\hat{x}_\theta = H^T_{P\theta}(R_P)^{-1}[z_P - h_P\ (\hat{x}^i_\theta, \hat{x}^i_V)] \tag{5}$$

$$\hat{x}_\theta^{i+1} = \hat{x}_\theta{}^i + \Delta\hat{x}_\theta \tag{6}$$

$$G^{md}_{QV}\Delta\hat{x}_V = H^T_{QV}(R_Q)^{-1}[z_Q - h_Q\ (\hat{x}^{i+1}_\theta, \hat{x}^i_V)] \tag{7}$$

$$\hat{x}_V^{i+1} = \hat{x}_V^i + \Delta\hat{x}_V \tag{8}$$

where $\hat{x}_\theta$ and $\hat{x}_V$ are the active and reactive state vectors composed by the voltage phase angles and magnitudes, respectively, i indicates the iteration number, and

$$G_{P\theta}^{md} = H_{P\theta}^T (R_P)^{-1} H_{P\theta} \tag{9}$$

$$G_{QV}^{md} = H_{QV}^T (R_Q)^{-1} H_{QV} \tag{10}$$

Also known as Model Decoupled Estimator (MD-SE) [16], this fast-decoupled approach impacts both sides of the original problem solution in (3), imposing inaccuracies in the problem solution. As discussed in the literature, the difference in the results obtained via MD-SE is acceptable for real-time operation purposes, provided that the decoupling effect is observable (high X/R ratios) [16], [3], [17].

This work investigated the impacts of MD-SE approaches when applied to electrical networks equipped with FACTS devices. As will be discussed in the results, the accuracy and convergence characteristics of the MD-SE are maintained when an extended formulation encompassing the inclusion of the shunt-type FACTS devices in the grid model is devised. However, this is not the case when incorporating series-type devices, where convergence is not always guaranteed. To circumvent these degrading effects while processing networks with series FACTS, this work proposes an alternative fast-decoupled method, as discussed next.

The new approach is based on the algorithm decoupled SE, where the decoupling is applied directly in the gain matrix, by disregarding the effect of the off-diagonal sub-matrices G_{PV} and $G_{Q\theta}$ (see (4)). In this case, the Jacobian matrix in (4), can be kept fully coupled, preventing the effects of the decoupling over the right-hand side vector of the state estimation solution in (3). The $H(\hat{x})$ matrix can be computed at each iteration, thus providing an exact solution. However, to reduce the computational burden of matrix $H(\hat{x})$ computation, this paper proposes a *modified* algorithm fast-decoupled approach, hereinafter referred to as MAD-SE, where the $H(\hat{x})$ is kept fully coupled but computed at flat-start and maintained constant during the whole iterative process. Since sub-matrices G_{PV} and $G_{Q\theta}$ are neglected, the desired decoupling between the active and reactive sub-problems is ensured. Solutions for $\Delta\theta$ and ΔV are computed efficiently via MD-SE or MAD-SE since in both cases the decoupled gain sub-matrices have half the size of the fully coupled gain matrix, and their triangular factors are computed only once at the beginning of the iterative solution. The active and reactive sub-problems are solved sequentially, as follows:

Modified Algorithm-Decoupled SE (MAD-SE):

$$G_{P\theta}^{mad}\Delta\hat{x}_\theta = \left[\ H_{P\theta}^T \mid H_{Q\theta}^T\ \right] R^{-1}[z - h(\hat{x}_\theta^i, \hat{x}_V^i)] \tag{11}$$

$$\hat{x}_\theta^{i+1} = \hat{x}_\theta^i + \Delta\hat{x}_\theta \tag{12}$$

$$G_{QV}^{mad}\Delta\hat{x}_\theta = \left[\ H_{PV}^T \mid H_{QV}^T\ \right] R^{-1}[z - h(\hat{x}_\theta^{i+1}, \hat{x}_V^i)] \tag{13}$$

$$\hat{x}_V^{i+1} = \hat{x}_V^i + \Delta\hat{x}_V \tag{14}$$

where:

$$G_{P\theta}^{mad} = H_{P\theta}^T (R_P)^{-1} H_{P\theta} + H_{Q\theta}^T (R_Q)^{-1} H_{Q\theta} \tag{15}$$

$$G_{QV}^{mad} = H_{PV}^T (R_P)^{-1} H_{PV} + H_{QV}^T (R_Q)^{-1} H_{QV} \tag{16}$$

III. Fast-Decoupled State Estimation with FACTS

As mentioned before, fast-decoupled WLS state estimation is widely applied in the industry thanks to its high computational efficiency, an essential feature for ensuring the network's real-time modelling [16], [3]. This section presents the proposed approach that extends the decoupled approaches described in Section II to include electrical models of FACTS devices, which is, as far as we know, a gap in the area. This update aims to preserve the reliability of the results while bringing the well-known and desired accuracy and computational efficiency of the fast-decoupled approach for the state estimation of networks with embedded FACTS devices. It is worth noting that the addition of new state variables to represent the controller variable is followed by the addition of an equal number of virtual measurements that represent the controlled quantities. This means that the network degrees of freedom are not affected by the proposed FACTS representation, so the same level of redundancy as conventional state estimation is required to ensure observability.

In the following sections, the electrical models proposed for each FACTS type and their impact on the decoupled approaches are presented.

A. Static VAR Compensator (SVC)

The SVC is a shunt-type device capable of regulating the voltage level at the bus k where it is connected. From an operational (steady-state) point of view, it behaves similarly to a variable susceptance which, according to its characteristic, inductive or capacitive, generates or absorbs reactive power to control the voltage magnitude at bus k [2]. Fig. 1 illustrates the equivalent electrical model of the SVC [18].

The SVC contribution to the reactive power injection at bus k, is given by:

$$Q_{SVC} = -V_k^2 b_{SVC} \tag{17}$$

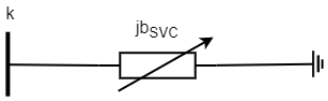

Fig. 1. SVC electric model.

Assuming a lossless operation, SVC only impacts the reactive part of the formulation. Accordingly, the SVC susceptance b_{SVC} is included as a new reactive state variable, extending the reactive partition of the state vector, as shown in (18), while the active counterpart remains unchanged.

$$\hat{x}_V^{ext} = \left[\ \hat{V} \quad \hat{b}_{SVC}\ \right]^T \tag{18}$$

where $\hat{V}$ is the reactive state vector, composed by the bus voltage magnitudes at all buses.

The estimation of the controller variable is then carried out together with the bus voltage magnitude in the reactive solution. It is worth noticing that the specified value for V_k is represented by a virtual reactive measurement in an accordingly enlarged z_Q vector, keeping unchanged the network degrees of freedom.

The extended reactive state vector in (18) impacts only the reactive partitions of the decoupled Jacobian matrix in (4), that is, $H_{P\theta}$ and $H_{Q\theta}$ remain unchanged, while H_{PV} and H_{QV} are extended to:

$$H_{PV}^{ext} = \left[\begin{array}{cc} H_{PV} & 0 \end{array} \right] \qquad H_{QV}^{ext} = \left[\begin{array}{cc} H_{QV} & \frac{\partial h_Q}{\partial b_{SVC}} \end{array} \right] \quad (19)$$

The SVC estimated susceptance is computed at every 1/2 reactive iteration by either the MD-SE, by applying the extended arrays in (5-8), or MAD-SE, by applying the solution represented in (11-14).

B. Static Synchronous Compensator (STATCOM)

As for the SVC, the STATCOM is capable of regulating the voltage magnitude at the bus k where it is connected. However, its basic structure can be synthesized by an electronically adjustable voltage source connected to the electrical network through a coupling transformer, represented by a constant susceptance, b_{STT}, as shown in the steady-state equivalent model illustrated in Fig. 2 [18], [2].

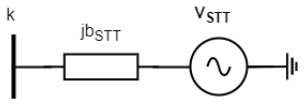

Fig. 2. STATCOM electric model.

As a lossless operation is assumed, the voltage angular difference between the STT source and bus k is equal to zero, that is, $\theta_{STT} = \theta_k$. Meanwhile, the reactive power absorbed or generated by the controller at bus k is produced by the difference between the voltage magnitudes of its source, V_{STT}, and at bus k, that is:

$$Q_{STT} = -V_k^2 b_{STT} + V_{STT} V_k b_{STT} \quad (20)$$

For the proposed fast-decoupled approaches, the controller voltage magnitude, V_{STT}, is included as a new reactive state variable, while the specified value for the controlled variable V_k is included as a virtual measurement in an enlarged vector z_Q. The extended reactive state vector is given by:

$$\hat{x}_V^{ext} = \left[\begin{array}{cc} \hat{V} & \hat{V}_{STT} \end{array} \right]^T \quad (21)$$

The extended vector (21) implies in an additional column in submatrices H_{PV} and H_{QV} in (4), that is:

$$H_{PV}^{ext} = \left[\begin{array}{cc} H_{PV} & 0 \end{array} \right] \qquad H_{QV}^{ext} = \left[\begin{array}{cc} H_{QV} & \frac{\partial h_Q}{\partial V_{STT}} \end{array} \right] \quad (22)$$

As for the SVC, the model and algorithm decoupled versions of the FD-SE described in Section II can be applied. The STATCOM voltage estimate is then updated after every 1/2 reactive iteration by applying the extended arrays in the solution represented by (5-8), if MD-SE is chosen, or in (11-14), in the case of the MAD-SE approaches.

C. Static Synchronous Series Compensator (SSSC)

Different from SVC and STACOM, the SSSC is a series-type device capable of controlling the active and/or reactive power flow through the transmission line where it is connected. This control effect is due to its ability to produce balanced alternating voltages, at nominal frequency, with controllable amplitude and phase angle [18]. The steady-state equivalent model of the SSSC is shown in Fig. 3.

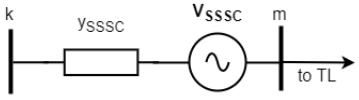

Fig. 3. SSSC electric model.

The $\boldsymbol{V_{SSSC}}$ in Fig. 3 is the complex voltage of the controllable source that produces the power flow control effects, and b_{SSSC} is the susceptance of the transformer that couples the SSSC to the transmission line (TL). The active and reactive power flow expressions, assuming $k - m$ the terminal buses of the SSSC, with m being the point of the series connection between the controller and the TL, are given by:

$$\begin{aligned} P_{mk} &= g_{sssc}(V_m)^2 \\ &- V_k V_m [g_{sssc} cos(\theta_m - \theta_k) + b_{sssc} sin(\theta_m - \theta_k)] \\ &+ V_m V_{sssc} [g_{sssc} cos(\theta_m - \theta_{sssc}) + b_{sssc} sin(\theta_m - \theta_{sssc})] \end{aligned} \quad (23)$$

$$\begin{aligned} Q_{mk} &= -b_{sssc}(V_m)^2 \\ &- V_k V_m [g_{sssc} sin(\theta_m - \theta_k) - b_{sssc} cos(\theta_m - \theta_k)] \\ &+ V_m V_{sssc} [g_{sssc} sin(\theta_m - \theta_{sssc}) - b_{sssc} cos(\theta_m - \theta_{sssc})] \end{aligned} \quad (24)$$

In the proposed fast-decoupled approaches, the desired/specified values for the active and reactive power flow through the TL, as well as the null active and reactive injection at the connection node m, are included as virtual active and reactive measurements in the corresponding vectors z_P and z_Q.

It should be stressed that the active and reactive state vectors are extended to include the SSSC voltage phase angle and magnitude as new state variables, that is:

$$\hat{x}_\theta^{ext} = \left[\begin{array}{cc} \hat{\theta} & \hat{\theta}_{SSSC} \end{array} \right]^T \qquad \hat{x}_V^{ext} = \left[\begin{array}{cc} \hat{V} & \hat{V}_{SSSC} \end{array} \right]^T \quad (25)$$

The presence of the SSSC impacts all partitions of the Jacobian matrix H in (4), which are extended to:

$$H_{P\theta}^{ext} = \left[\begin{array}{cc} H_{P\theta} & \frac{\partial h_P}{\partial \theta_{SSSC}} \end{array} \right] \qquad H_{Q\theta}^{ext} = \left[\begin{array}{cc} H_{Q\theta} & \frac{\partial h_Q}{\partial \theta_{SSSC}} \end{array} \right] \quad (26)$$

$$H_{PV}^{ext} = \left[\begin{array}{cc} H_{PV} & \frac{\partial h_P}{\partial V_{SSSC}} \end{array} \right] \qquad H_{QV}^{ext} = \left[\begin{array}{cc} H_{QV} & \frac{\partial h_Q}{\partial V_{SSSC}} \end{array} \right] \tag{27}$$

The controller active state variables are computed iteratively, being θ_{SSSC} updated every 1/2 active iteration, and the variable V_{SSSC} updated every 1/2 reactive iteration, along with conventional active and reactive state variables, by using one of the fast-decoupled approaches, named MD-SE and MAD-SE (see Section II).

D. Unified Power Flow Controller (UPFC)

The UPFC is the most versatile among the FACTS devices due to its capability to bring together the functionalities of previously mentioned devices. The UPFC model for steady-state analysis can be seen as the association of SSSC and STATCOM models as illustrated in Fig. 4 [19].

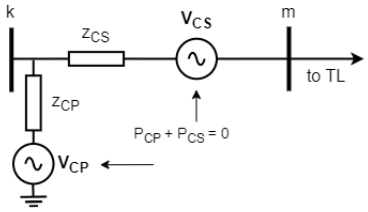

Fig. 4. UPFC electric model.

As for the former controllers, the active and reactive state vectors are extended to accommodate, along with the conventional state variables, the complex voltages associated with the UPFC, that is:

$$\hat{x}_P^{ext} = \left[\begin{array}{ccc} \theta_k & \theta_{cs} & \theta_{cp} \end{array} \right]^T \tag{28}$$

$$\hat{x}_Q^{ext} = \left[\begin{array}{ccc} V_k & V_{cs} & V_{cp} \end{array} \right]^T \tag{29}$$

where V_{cs} and θ_{cs} are the series voltage magnitude and phase angle, respectively, while V_{cp} and θ_{cp} are the parallel voltage magnitude and phase angle.

The two possible functionalities due to shunt and series association lead to contribution in the active and reactive power injection at bus k, and to the active and reactive power flows through the associated TL, as shown in (30-35).

$$\begin{aligned} P_k = (V_k)^2(g_{cs}+g_{cp}) \\ -V_kV_m[g_{cs}cos(\theta_k-\theta_m)+b_{cs}sin(\theta_k-\theta_m)] \\ -V_kV_{cs}[g_{cs}cos(\theta_k-\theta_{cs})+b_{cs}sin(\theta_k-\theta_{cs})] \\ -V_kV_{cp}[g_{cp}cos(\theta_k-\theta_{cs})+b_{cp}sin(\theta_k-\theta_{cp})] \end{aligned} \tag{30}$$

$$\begin{aligned} Q_k = -(V_k)^2(b_{cs}+b_{cp}) \\ -V_kV_m[g_{cs}sin(\theta_k-\theta_m)-b_{cs}cos(\theta_k-\theta_m)] \\ -V_kV_{cs}[g_{cs}sin(\theta_k-\theta_{cs})-b_{cs}cos(\theta_k-\theta_{cs})] \\ -V_kV_{cp}[g_{cp}sin(\theta_k-\theta_{cs})-b_{cp}cos(\theta_k-\theta_{cp})] \end{aligned} \tag{31}$$

$$\begin{aligned} P_m = (V_m)^2g_{cp} \\ -V_kV_m[g_{cs}cos(\theta_m-\theta_k)+b_{cs}sin(\theta_m-\theta_k)] \\ -V_mV_{cs}[g_{cp}cos(\theta_m-\theta_{cs})+b_{cp}sin(\theta_m-\theta_{cs})] \end{aligned} \tag{32}$$

$$\begin{aligned} Q_m = -(V_m)^2b_{cp} \\ -V_kV_m[g_{cs}sin(\theta_m-\theta_k)+b_{cs}cos(\theta_m-\theta_k)] \\ -V_mV_{cs}[g_{cp}sin(\theta_m-\theta_{cs})-b_{cp}cos(\theta_m-\theta_{cs})] \end{aligned} \tag{33}$$

$$\begin{aligned} P_{mk} = g_{cs}(V_m)^2 \\ -V_kV_m[g_{cs}cos(\theta_m-\theta_k)+b_{cs}sin(\theta_m-\theta_k)] \\ +V_mV_{cs}[g_{cs}cos(\theta_m-\theta_{cs})+b_{cs}sin(\theta_m-\theta_{cs})] \end{aligned} \tag{34}$$

$$\begin{aligned} Q_{mk} = -b_{cs}(V_m)^2 \\ -V_kV_m[g_{cs}sin(\theta_m-\theta_k)-b_{cs}cos(\theta_m-\theta_k)] \\ +V_mV_{cs}[g_{cs}sin(\theta_m-\theta_{cs})-b_{cs}cos(\theta_m-\theta_{cs})] \end{aligned} \tag{35}$$

In (30) to (35), as well as in Fig. 4, the subscript cs refers to the serial part of the controller and its parameters and the subscript cp refers to the shunt or parallel part of the controller and, likewise, its parameters.

Furthermore, the active power demanded by the series converter, P_{cs}, is supplied by the parallel converter, P_{cp}, through a coupling capacitor, a condition established for a lossless operation [2], which is expressed by:

$$P_p = P_{cs} + P_{cp} = 0 \tag{36}$$

where

$$\begin{aligned} P_{cs} = g_{cs}(V_{cs})^2 \\ -V_{cs}V_k[g_{cs}cos(\theta_{cs}-\theta_k)+b_{cs}sen(\theta_{cs}-\theta_k)] \\ +V_{cs}V_k[g_{cs}cos(\theta_{cp}-\theta_k)+b_{cs}sen(\theta_{cp}-\theta_k)] \end{aligned} \tag{37}$$

$$\begin{aligned} P_{cp} = g_{cp}(V_{cp})^2 \\ -V_{cp}V_k[g_{cp}cos(\theta_{cp}-\theta_k)+b_{cp}sen(\theta_{cp}-\theta_k)] \end{aligned} \tag{38}$$

The controller operational constraint represented by (36) is included in the FD-SE formulation by a null virtual active measurement in an enlarged z_P, along with the specified value of the active power flow, whose function is represented by P_{mk}. As for the specified values of voltage magnitude at bus k and the reactive power flow represented by Q_{mk}, they are included as new measurements in an enlarged vector z_Q.

The extended active and reactive state vectors in (28), (29) and the distinct virtual measurement in (36), as described above, impacts the decoupled Jacobian submatrices in (4), which are extended as follows:

$$H_{P\theta}^{ext} = \left[\begin{array}{ccc} H_{P\theta} & \frac{\partial h_P}{\partial \theta_{cs}} & \frac{\partial h_P}{\partial \theta_{cp}} \\ \\ \frac{\partial P_p}{\partial \theta} & \frac{\partial P_p}{\partial \theta_{cs}} & \frac{\partial P_p}{\partial \theta_{cp}} \end{array} \right] \tag{39}$$

$$H_{Q\theta}^{ext} = \left[\begin{array}{ccc} H_{Q\theta} & \frac{\partial h_Q}{\partial \theta_{cs}} & \frac{\partial h_Q}{\partial \theta_{cp}} \end{array} \right] \tag{40}$$

$$H_{PV}^{ext} = \begin{bmatrix} H_{PV} & \frac{\partial h_P}{\partial V_{cs}} & \frac{\partial h_P}{\partial V_{cp}} \\ \\ \frac{\partial P_p}{\partial V} & \frac{\partial P_p}{\partial V_{cs}} & \frac{\partial P_p}{\partial V_{cp}} \end{bmatrix} \quad (41)$$

$$H_{QV}^{ext} = \begin{bmatrix} H_{QV} & \frac{\partial h_Q}{\partial V_{cs}} & \frac{\partial h_Q}{\partial V_{cp}} \end{bmatrix} \quad (42)$$

The controller estimated phase angles, $\hat{\theta}_{cs}$ and $\hat{\theta}_{cp}$, are updated in the active 1/2 iteration, and controller estimated voltage magnitudes, $\hat{V}_{cs}$ and $\hat{V}_{cp}$, are updated in the reactive 1/2 iteration, respectively. As for the previous controllers, the decoupled modelling proposed for the UPFC is incorporated into the MD-SE and MAD-SE described in Section II.

E. Controller state variables initialization

The flat starting condition, applied to the complex bus voltages in the Jacobian matrix computation, is not always effective for the initialization of controller variables. An inadequate choice of these values may compromise the convergence of decoupled methods and even WLS-SE. In this work, the controller variable initial values follow the proposal in [18], defined as follows. For the shunt SVC controllers, $b_{SVC}^0 = 0$, which corresponds to the device's resonance point. The flat-start condition to STATCOM source voltage is adopted.

For series controllers, the initial values for its source magnitude and phase angle are written as a function of the specified values attributed to active and reactive power flow, as follows:

$$|V_{SSSC}| = X_{SSSC}\sqrt{\left(P_{mk}^{specif}\right)^2 + (Q_{mk}^{specif})^2} \quad (43)$$

$$\theta_{SSSC} = arctan|(P_{mk}^{specif})/(Q_{mk}^{specif})| \quad (44)$$

For the UPFC, the same conditions of shunt and serial controllers are adopted.

IV. Simulation Results

The proposed approaches for fast-decoupled state estimation with embedded FACTS devices, described in Sections II and III (MD-SE and MAD-SE), have been coded and tested in the IEEE 30 bus system under distinct FACTS operation scenarios. The measurement plan includes bus voltage magnitudes, active and reactive power injections, and active and reactive power flows in all branches, as well as the virtual measurements corresponding to each type of FACTS device, so that system observability is ensured.

The measurement values are generated by adding zero means Gaussian noise to the exact solution corresponding to the power flow (PF) method described in [2]. The standard deviation values (σ) are set as in [3], i.e., $8\cdot10^{-3}$, $1\cdot10^{-2}$ and $4\cdot10^{-3}$ for power flow, power injection and voltage magnitude measurements, respectively.

The results obtained with the proposed decoupled approaches are compared with the exact solution obtained with the PF, as well as with values estimated from a coupled WLS estimator, endowed with the same ability to process FACTS devices (hereinafter referred to as WLS-SE).

Given the random nature of measurement noises, Monte Carlo simulations are performed for all cases presented. The Mean Average Error (MAE) is used to infer the proposal's accuracy. MAE is computed for each state variable according to (45). The smaller the MAE, the better the estimated state fits the measurements [20].

$$MAE = \frac{1}{N_{st}\cdot N_{MC}} \sum_{i=1}^{N_{st}} \sum_{m=1}^{N_{MC}} \left| \frac{x_i^{ref} - \hat{x}_i}{x_i^{ref}} \right| \quad (45)$$

where N_{st} is the number of state variables, N_{MC} is the number of Monte Carlo Simulations, x_i^{ref} is the reference value of the state variable *i*, obtained from the exact PF solution, and $\hat{x}_i$ the estimated value of the state variable *i*.

In the following, the results for one random simulation with noise measurements are presented, along with the computed MAE corresponding to 2000 Monte Carlo simulations. The convergence tolerance for all state estimators is set as 10^{-4}. All methods have been coded in MATLAB™. Due to the space restriction, in all cases, only the results of the controllers' state variables are presented. The acronym NC in the tables refers to Non-Convergent.

A. Shunt-type Controllers

1) SVC Case: in this case, an SVC was installed at bus 7 of the 30-bus test system with a specified control voltage magnitude of 1pu, which is included as a reactive virtual measurement, as discussed in Section III.

Table I presents the computed value of the controller state variable, b_{SVC}, obtained with the PF, as well the estimated values from WLS-SE, MD-SE, and MAD-SE, alongside their respective number of iterations (n_{it}). In this case, the estimated value of b_{SVC} obtained with both MD-SE and MAD-SE are very close to that provided by the exact values of the PF, as is the estimate provided by the coupled WLS-SE.

Regarding the number of iterations, the WLS-SE methodology converges into 3 (*full*) iterations, while the MD- and the MAD-SE require 6 and 4 iterations, respectively. This is an excellent result since each iteration of the decoupled methods has a drastic reduction in computational burden thanks to the constant and decoupled Gain matrix, as discussed in Section II. This is valid for all future cases and will be omitted for the sake of brevity.

TABLE I
Results of the Decoupled Methods for the SVC

Data	PF	WLS-SE	MD-SE	MAD-SE
b_{SVC}	0.3477	0.3474	0.3474	0.3474
n_{it}	4	3	6	4

Table II presents the MAE obtained with the Monte Carlo Simulations for the SVC case. It is observed the decoupled approaches (MD- and MAD-SE) possess comparable results with the WLS-SE, attesting to the accuracy of the proposed decoupled methods.

TABLE II
MAE RESULTS FOR SVC-CASE

Data	WLS-SE	MD-SE	MAD-SE
V	6.83E-04	7.06E-04	6.75E-04
θ	1.33E-03	3.09E-03	1.30E-03
b_{SVC}	1.54E-03	1.66E-03	1.53E-03

2) STATCOM Case: : a STATCOM was installed at bus 19, with a couple of transformer reactance equal to 0.1 pu, as in [2]. The voltage at bus 19 is set to 1 pu.

It is seen, from the results presented in Table III, that only a minimum deviation from the exact value is perceived when applying the MD-SE and the MAD-SE, and even smaller when compared to the WLS-SE, as expected. As for the number of iterations, excellent results are obtained, with MD-SE and MAD-SE requiring 6.5 and 4.5 iterations (with constant and half-size matrices), respectively, against 4 full iterations of the WLS-SE.

The MAE corresponding to the Monte Carlo simulations, presented in Table IV, attest the accuracy of the estimated values obtained with the decoupled approaches (MD- and MAD-SE) and indicate a performance equivalent to that of the coupled WLS-SE method.

TABLE III
RESULTS OF THE DECOUPLED METHODS FOR THE STATCOM

Data	PF	WLS-SE	MD-SE	MAD-SE
V_{STT}	1.0181	1.0184	1.0184	1.0183
n_{it}	4	4	6.5	4.5

TABLE IV
MAE RESULTS FOR STATCOM-CASE

Data	WLS-SE	MD-SE	MAD-SE
V	6.77E-04	6.90E-04	6.86E-04
θ	1.37E-03	3.25E-03	1.38E-03
V_{STT}	5.65E-04	5.79E-04	5.80E-04

B. Series-type Controller: SSSC-Case

In this case, an SSSC controller was installed in series with the transmission line located between buses 6-28 of the test system, aiming to provide active and reactive power flow control through it. The value assigned to the SSSC coupling transformer reactance is 0.7 pu, as is also adopted in [4]. The specified power flow targets for the SSSC are $P_{mk} = 0.73$ MW and $Q_{mk} = 1.67$ MVAr.

Table V presents the exact and estimated values of the controller state variables. The proposed MD- and MAD-SE achieve values very close to the exact solution via PF for the magnitude and phase angle of the controller. In terms of the number of iterations, MD- and MAD-SE require 6.5 and 12.5 iterations versus 6 full iterations of the WLS-SE. Although it is a larger increase than the shunt-types controllers, the decoupled approaches' computational simplicity leans towards a reduction in floating point operations, thanks to the use of half-sized constant matrices versus the full Jacobian matrix. Table VI presents the MAE obtained with the Monte Carlo analysis for the SSSC-Case. Again the proposed decoupled approaches (MD- and MAD-SE) possess comparable results with WLS-SE, attesting their accuracy.

TABLE V
RESULTS OF THE DECOUPLED METHODS FOR THE SSSC

Data	PF	WLS-SE	MD-SE	MAD-SE
V_{SSSC}	0.0112	0.0111	0.0110	0.0111
θ_{SSSC}	28.5820°	27.8720°	29.1663°	28.1114°
n_{it}	5	6	6.5	12.5

TABLE VI
MAE RESULTS FOR SSSC-CASE

Data	WLS-SE	MD-SE	MAD-SE
V	6.85E-04	7.04E-04	7.06E-04
θ	1.38E-03	3.52E-03	1.39E-03
V_{SSSC}	1.95E-02	1.58E-02	1.89E-02
θ_{SSSC}	2.47E-02	3.44E-02	2.35E-02

C. Series-shunt type Controller: UPFC Case

In this case, a UPFC was installed at bus 4, in series with the transmission line 4-6. The series and parallel reactances are both assumed as 0.1 pu, as set in [6]. The specified values for the active and reactive power flow through the TL are set as $P_{mk} = -21.31$ MW and $Q_{mk} = -10.56$ MVAr, and the specified voltage for bus 4 is set as 1 pu, therefore contemplating the entire device's control capacity.

Table VII summarizes the results regarding the phase angle and magnitude of the UPFC complex voltages. Differently from previous cases, the MD-SE algorithm is unable to reach convergence, as shown in the fourth column of the table. However, the proposed modified approach, MAD-SE was capable of appropriately estimating the UPFC's operating point, reaching very close values to the exact ones provided by the PF and to the estimated values obtained with the WLS-SE. The MAD-SE required 13 iterations to achieve convergence against 4 of the WLS-SE. These results need to be analysed in light of the high computational cost of calculation of the fully coupled Jacobian matrix and Gain matrix factorization required by the WLS-SE. Therefore, the computational superiority of decoupled methods will be more significant the larger the size of the network under study, as they work with constant decoupled matrices. Also for the UPFC-Case, the MAE results, shown in Table VIII, attest the accuracy of the proposed MAD-SE.

D. Multiple FACTS Case

In this case, the UPFC installed in subsection IV.D was preserved and, additionally, an SVC was installed at bus 20 and a STATCOM at bus 14, both to increase the voltage levels at the connection points to 1 pu. The results are summarized in Table IX. As for the UPFC-Case, convergence is not achieved when the MD-SE algorithm is used, reinforcing the importance

TABLE VII
RESULTS OF THE DECOUPLED METHODS FOR THE UPFC

Data	PF	WLS-SE	MD-SE	MAD-SE
V_{cs}	0.0261	0.0262	NC	0.0262
θ_{cs}	-68.7349°	-68.4257°	NC	-69.5028°
V_{cp}	1.0248	1.0255	NC	1.0253
θ_{cp}	-2.0117°	-2.0084°	NC	-2.0137°
n_{it}	4	4	NC	13

TABLE VIII
MAE RESULTS FOR UPFC-CASE

Data	WLS-SE	MD-SE	MAD-SE
V	7.03E-04	NC	6.86E-04
θ	1.36E-03	NC	1.70E-03
V_{cs}	2.82E-03	NC	2.78E-03
θ_{cs}	5.46E-03	NC	1.58E-02
V_{cp}	5.90E-04	NC	6.01E-04
θ_{cp}	1.24E-03	NC	2.68E-03

of the proposed modified approach, the MAD-SE, that again ensures convergence. The good performance of the MAD-SE observed in all previous cases is preserved in the presence of multiple FACTS devices, with estimated values equal to or very close to those provided by the exact PF and estimated by WLS-SE. When it comes to the number of iterations, MAD-SE requires 12 iterations, maintaining the same pattern seen in the previous simulation. MAE are computed and shown in Table X. Again the values obtained with the decoupled approach MAD-SE possess comparable results with WLS-SE, attesting the accuracy of the proposed method even in the presence of multiple types of FACTS.

TABLE IX
RESULTS OF THE DECOUPLED METHODS FOR THE MULTIPLE FACTS

Data	PF	WLS-SE	MD-SE	MAD-SE
b_{SVC}	0.1573	0.1578	NC	0.1577
V_{STT}	1.0088	1.0088	NC	1.0087
V_{cs}	0.0255	0.0254	NC	0.0255
θ_{cs}	-72.6111°	-73.1595°	NC	-74.5225°
V_{cp}	1.0222	1.0227	NC	1.0224
θ_{cp}	-2.0259°	-2.0243°	NC	-2.0311°
n_{it}	4	4	NC	12

TABLE X
MAE RESULTS FOR MULTIPLE FACTS CASE

Data	WLS-SE	MD-SE	MAD-SE
V	6.80E-04	NC	6.72E-04
θ	1.33E-03	NC	1.82E-03
b_{SVC}	4.12E-03	NC	4.30E-03
V_{STT}	4.97E-04	NC	5.39E-04
V_{cs}	2.66E-03	NC	3.13E-03
θ_{cs}	5.52E-03	NC	1.76E-02
V_{cp}	5.79E-04	NC	6.01E-04
θ_{cp}	1.21E-03	NC	3.01E-03

E. Computation Time - Comparative Results

This section presents a relative computation time (RCT) for decoupled approaches and the coupled WLS-SE method. All processing times were compared with the computation time, T_0, required by the traditional coupled WLS-SE, with no FACTS devices. As shown in Table XI, there is a significant increase in the computation time when the network contains FACTS, especially in the cases with series FACTS-based components. The decoupled approaches can alleviate this effect when compared to the coupled WLS-SE approach, especially when shunt FACTS-based components are considered. Also, MAD-SE presents lower RCT than the WSL-SE in all scenarios. It is noteworthy that the larger the size of the network under study, the more significant the computational superiority of decoupled methods, as they work with constant decoupled matrices as discussed previously.

TABLE XI
RELATIVE COMPUTATIONAL TIME

Case	WLS-SE	MD-SE	MAD-SE
A1	1.22 T_0	0.91 T_0	0.60 T_0
A2	1.60 T_0	0.92 T_0	0.65 T_0
B	2.70 T_0	1.16 T_0	2.41 T_0
C	2.27 T_0	NC	1.74 T_0
D	2.32 T_0	NC	1.72 T_0

V. CONCLUSIONS

This work extends the computational benefits and accuracy of the decoupled state estimation method, widely accepted and employed in operation centres around the world, for the processing of networks equipped with FACTS devices. Two extended decoupled methods are proposed: an extended model decoupled SE, MD-SE, and a modified algorithm decoupled SE, MAD-SE.

The simulation results, which are compared with those obtained by an exact power flow and a coupled WLS-SE, demonstrate that the proposed approaches are capable of accurately estimating the conventional system state variables (complex bus voltages), alongside the controllers' state variables of different FACTS devices. The results also indicate that the MAD-SE algorithm presents superior robustness than the MD-SE by ensuring convergence in all cases, while also preserving the same level of accuracy as the coupled WLS-SE. Although an increase in the number of iterations in decoupled methods is expected, a reduction in computational burden is achieved due to the simplifications and reduction in size resulting from the decoupling applied to the Jacobian and/or Gain matrices, potentially improving their real-time applications.

REFERENCES

[1] N. Hingorani and L. Gyugyi, *Understanding FACTS: Concepts and Technology of Flexible AC Transmission Systems*. Wiley, 2000.

[2] E. Acha, C. R. Fuerte-Esquivel, H. Ambriz-Perez, and C. Angeles-Camacho, *FACTS: modelling and simulation in power networks*. New York: Wiley-Blackwell, 2004.

[3] A. Abur and A. G. Exposito, *Power system state estimation: theory and implementation*. CRC press, 2004.

[4] B. Xu and A. Abur, "State estimation of systems with embedded facts devices," in *2003 IEEE Bologna Power Tech Conference Proceedings,*, vol. 1. IEEE, 2003, pp. 5–pp.
[5] ——, "State estimation of systems with upfcs using the interior point method," *IEEE Transactions on Power Systems*, vol. 19, no. 3, pp. 1635–1641, 2004.
[6] A. Zamora-Cárdenas and C. R. Fuerte-Esquivel, "State estimation of power systems containing facts controllers," *Electric Power Systems Research*, vol. 81, no. 4, pp. 995–1002, 2011.
[7] A. d. l. V. Jaén, E. Acha, and A. G. Expósito, "Voltage source converter modeling for power system state estimation: STATCOM and VSC-HVDC," *IEEE transactions on power systems*, vol. 23, no. 4, pp. 1552–1559, 2008.
[8] V. B. Venkateswaran and V. Manoj, "State estimation of power system containing FACTS controller and PMU," in *2015 IEEE 9th International Conference on Intelligent Systems and Control (ISCO)*. IEEE, 2015, pp. 1–6.
[9] M. A. Chitsazan, M. S. Fadali, and A. M. Trzynadlowski, "State estimation of IEEE 14 bus with unified interphase power controller (UIPC) using WLS method," in *2017 IEEE Energy Conversion Congress and Exposition (ECCE)*. IEEE, 2017, pp. 2903–2908.
[10] E. Zamora-Cárdenas, B. Alcaide-Moreno, and C. Fuerte-Esquivel, "State estimation of flexible AC transmission systems considering synchronized phasor measurements," *Electric Power Systems Research*, vol. 106, pp. 120–133, 2014.
[11] V. I. Presada, C. V. Cristea, M. Eremia, and L. Toma, "State estimation in power systems with FACTS devices and PMU measurements," in *2014 49th International Universities Power Engineering Conference (UPEC)*. IEEE, 2014, pp. 1–5.
[12] W. Li and L. Vanfretti, "A PMU-based state estimator for networks containing VSC-HVDC links," in *2015 IEEE Power & Energy Society General Meeting*. IEEE, 2015, pp. 1–5.
[13] C. Rakpenthai, S. Premrudeepreechacharn, S. Uatrongjit, and N. R. Watson, "An interior point method for WLAV state estimation of power system with UPFCs," *International Journal of Electrical Power & Energy Systems*, vol. 32, no. 6, pp. 671–677, 2010.
[14] M. A. Chitsazan, M. S. Fadali, and A. M. Trzynadlowski, "State estimation for large-scale power systems and FACTS devices based on spanning tree maximum exponential absolute value," *IEEE Transactions on Power Systems*, vol. 35, no. 1, pp. 238–248, 2019.
[15] L. F. G. de Lima, O. L. Tortelli, E. M. Lourenço, and R. K. Portelinha, "Fast decoupled state estimation including thyristor controlled series compensator devices," *Electric Power Systems Research*, vol. 213, p. 108439, 2022.
[16] A. Monticelli, *State estimation in electric power systems: a generalized approach*. Springer Science & Business Media, 1999.
[17] E. M. Lourenço and J. B. A. London Jr, *Power Distribution System State Estimation*. IET, 2022.
[18] O. L. Tortelli, "Alocation and operation of facts controllers in electric power system *(in Portuguese)*," Ph.D. dissertation, UNICAMP - Universidade Estadual de Campinas, Campinas - Brazil, 2010.
[19] T. Okon and K. Wilkosz, "Consideration of different operation modes of UPFC in power system state estimation," in *2011 10th International Conference on Environment and Electrical Engineering*. IEEE, 2011, pp. 1–4.
[20] R. Schincariol da Silva, T. R. Fernandes, and M. C. de Almeida, "Specifying angular reference for three-phase distribution system state estimators," *IET Generation, Transmission & Distribution*, vol. 12, no. 7, pp. 1655–1663, 2018.